Hydrol. Earth Syst. Sci., 17, 1093–1111, 2013
www.hydrol-earth-syst-sci.net/17/1093/2013/
doi:10.5194/hess-17-1093-2013

Hydrology and Earth System Sciences
Open Access

Global hydrobelts and hydroregions: improved reporting scale for water-related issues?

M. Meybeck[1], **M. Kummu**[2], **and H. H. Dürr**[3]

[1]Centre National de la Recherche Scientifique (CNRS), University Pierre and Marie Curie, Paris, France
[2]Water & Development Research Group, Aalto University, Espoo, Finland
[3]Ecohydrology Research Group, Department of Earth and Environmental Sciences, University of Waterloo, Waterloo, ON, Canada

Correspondence to: M. Meybeck (michel.meybeck@upmc.fr)

Received: 13 July 2012 – Published in Hydrol. Earth Syst. Sci. Discuss.: 3 August 2012
Revised: 12 February 2013 – Accepted: 12 February 2013 – Published: 13 March 2013

Abstract. Global-scale water issues such as its availability, water needs or stress, or management, are mapped at various resolutions and reported at many scales, mostly along political or continental boundaries. As such, they ignore the fundamental heterogeneity of hydroclimates and natural boundaries of river basins. Here we describe the continental landmasses at two levels: eight hydrobelts strictly limited by river basins, defined at a 30′ (0.5°) resolution, which are decomposed on continents as 26 hydroregions. The belts were defined and delineated, based primarily on the annual average temperature (T) and run-off (q), to maximise inter-belt differences and minimise intra-belt variability.

This new global puzzle defines homogeneous and near-contiguous entities with similar hydrological and thermal regimes, glacial and postglacial basin histories, endorheism distribution and sensitivity to climate variations. The mid-latitude, dry and subtropical belts have northern and southern analogues and a general symmetry can be observed for T and q between them. The boreal and equatorial belts are unique. Population density between belts and between the continents varies greatly, resulting in pronounced differences between the belts with analogues in both hemispheres.

Hydroregions (median size 4.7 M km^2) are highly contrasted, with the average q ranging between 6 and 1393 mm yr^{-1} and the average T between −9.7 and +26.3 °C, and a population density ranging from 0.7 to 0.8 p km^{-2} for the North American boreal region and some Australian hydroregions to 280 p km^{-2} for some Asian hydroregions. The population/run-off ratio, normalised to a reference pristine region, is used to map and quantify the global population at risk of severe water quality degradation. Our initial tests suggest that hydrobelt and hydroregion divisions are often more appropriate than conventional continental or political divisions for the global analysis of river basins within the Earth system and of water resources.

The GIS files of the hydrobelts and hydroregions are available at the supplement of this article and at doi:10.1594/PANGAEA.806957 as well as geotypes.net.

1 Introduction

Mapping global water resources was first done for precipitation and run-off; the maps were at a very coarse resolution due to sparsely available data, a lack of global models and a lack of satellite imagery. In 1964 the Soviet Academy of Science in Moscow issued a novel work, the *Physico-geographic Atlas of the World* (Gerasimov et al., 1964), which presented a similar set of maps for precipitation and run-off for each continent and for the Soviet Union. The maps included relief, geology, climate, vegetation, etc., at an unprecedented resolution (1/20 000 000). In 1975 Baumgartner and Reichel published the World Water Balance with detailed maps and tables on precipitation, evaporation, and run-off for each continent as well as specific tables for latitudinal zones, and Soviet hydrologists (Korzoun et al., 1978) established for UNESCO another description of the water balance for each continent. Even though Baumgartner and Reichel (1975) considered drainage basins to oceans, ultimately none of these global-scale analyses took into account

the natural hydrographic entities delineated by river basins in their reporting and tabulations.

Global hydrology outputs have changed markedly in the last twenty years due to satellite imagery, global hydrological models and geographic information systems (GIS). Subsequently, these three tools have made it possible (i) to map the components of the hydrological balance at high resolution (Vörösmarty et al., 2000c; Fekete et al., 2002; Alcamo et al., 2003; Oki and Kanae, 2006); (ii) to delineate the surficial river networks and/or the boundaries of river basins at a global scale, first at 2° (two arc degrees; around 200 km at the equator) (Probst, 1992; Probst et al., 1997) then at 30′ (30 arc minutes or 0.5°; around 50 km at the equator) (Vörösmarty et al., 2000a, b; Oki and Kanae, 2006) and finer, and the lakes and wetland distributions (Lehner and Döll, 2004); (iii) to replace paper copies of the world hydrological atlases with digital geospatial maps at various resolutions (Vörösmarty et al., 2000a, b, c; Alcamo et al., 2003; Lehner and Döll, 2004; Oki and Kanae, 2006; van Beek et al., 2011); and (iv) to combine water resources with other numerical maps, particularly population maps, resulting in the analysis of water needs and availability at high resolutions (Vörösmarty et al., 2000c; Viviroli et al., 2007; Kummu et al., 2010; Wada et al., 2011).

The analysis of global water-related issues, needing discrete river basins as the analysis unit, is now commonly performed at 30′ resolution ($n = 60\,000$ cells, $n = 6200$ individual river basins) (Vörösmarty et al., 2000a, b) for global analyses and higher resolution for regional analysis or specific questions. When multiple issues need to be compared, various spatial delineations and/or reporting formats have been used; this has been done, for instance, for river water management using various scales: (i) continents (Kulshreshtha, 1998; Vörösmarty et al., 2000c; Rockström et al., 2009; Wada et al., 2011); (ii) economic and/or political regions (Falkenmark, 1997; Kulshreshtha, 1998; Arnell, 2004; Islam et al., 2007; Kummu et al., 2010); (iii) countries ($n = 100$ to 200 entities) (Sullivan et al., 2003; Falkenmark et al., 2009; World Water Assessment Programme, 2009); (iv) latitudinal bands (Baumgartner and Reichel, 1975; Kummu and Varis, 2011); and (v) climate (Köppen, 1931) and ecosystem bands (Holdridge, 1967). Other river aggregation has been done to assess the impact of dam construction ($n = 100$ to 1000) (Vörösmarty et al., 1997; Nilsson et al., 2005), as well as the hydro-ecoregions (Abell et al., 2008).

Global river systems are also considered for the analyses of the response of the Earth system under past, present and future global change (Talaue-McManus et al., 2003; Kabat et al., 2004; Steffen et al., 2004). Global river datasets were therefore assembled to map river inputs to coastal oceans for carbon and nutrients (e.g. Ludwig and Probst, 1998; Seitzinger et al., 2005, 2010; Dürr et al., 2011), and for sediments (Milliman and Farnsworth, 2011). Studies on aggregated river basins have been gradually regionalised, first for rivers discharging water into oceans at different latitudinal bands (Probst, 1992), then for homogeneous coastal zone catchments – termed COSCATs (Meybeck et al., 2006, 2007) – specific ocean basins, regional seas and estuarine types (Meybeck and Dürr, 2009; Laruelle et al., 2010; Dürr et al., 2011).

Similarly, the regionalisation of water-related issues has been increasingly studied based on more homogeneous hydro-climatic, political and/or socioeconomic regions. For instance, Asia has been divided into Eastern Asia, Southern Asia, Northern Asia and the Middle East using country aggregates (e.g. Kummu et al., 2010). Researchers have also recently clustered world river basins into 426 homogeneous ecoregions (Abell et al., 2008), with catchment areas ranging from 23 km^2 to 4.53 M km^2 (average 311 000 km^2) on the basis of their fish populations. The largest basins, which are more heterogeneous, are also fragmented, for example, into 13 ecoregions for the Amazon River basin (Abell et al., 2008).

Traditional global-scale reporting, however, faces multiple complications. Aggregating the results at a country level may smooth out major hydro-physical and social discrepancies for the largest countries, such as China, Russia, the US, Australia, Canada or Brazil. Furthermore, it is difficult to compare studies on different geopolitical entities when the political situation is evolving, such as for the European Union or the former USSR. It is also difficult to analyse a great number of entities just using tables: similarities and/or contrasts are not obvious when more than 50 entities are used, while they are masked if only a very small number of objects (e.g. six continents) are used. Natural hydrological boundaries, which delineate rivers basins, are now often stated to be more appropriate to analyse a society's water consumption behaviour and manage its water-related issues (Millennium Ecosystem Assessment, 2005; World Water Assessment Programme, 2009).

We postulate that both the analysis and tabulation of multiple water-related issues is better performed when using similarly defined permanent spatial entities, particularly when done on a global scale, rather than traditional reporting scales. We argue that *an analysis of global water issues can be improved and harmonised using a limited and fixed number of spatial entities that are delineated without compromising river basin boundaries*.

We thus propose to delineate the continental landmass into homogenous hydrological regions, the *hydrobelts*, which are formed with aggregated river basins and decomposed on continents as *hydroregions*. The goal is to define hydrobelts at a useable resolution that makes it possible to easily connect them to other databases at the same resolution. We consider less than thirty hydroregions, for which the physical characteristics, climate, hydrology, and life zones are first tabulated and compared. We then apply this new global-scale fragmentation to the population distribution and population pressure on river run-off at different spatial scales.

Table 1. Target limits of annual average temperature (T) and run-off (q) for aggregated river basins defining hydrobelts.

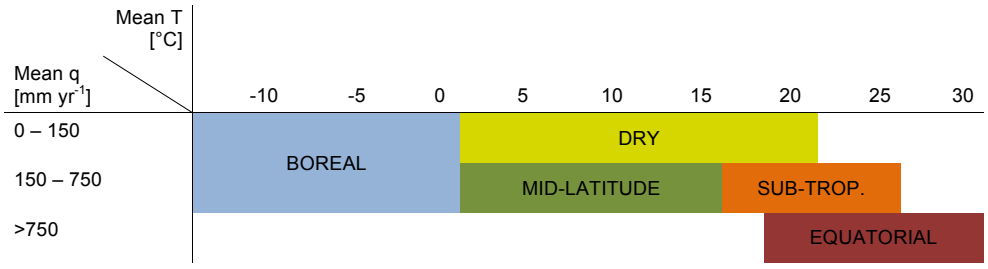

2 Hydrobelt delineation principles and datasets used

2.1 Principles of hydrobelt delineation

In order to facilitate mapping, reporting and analysis at a global scale, we defined hydrobelts to cross the continental borders, forming hydrologically homogenous regions, based on the following criteria:

1. hydrobelts are delineated by natural hydrological basins, which cannot be segmented (e.g. headwaters are not separated from lowlands);

2. belts are defined based on their average water balance attributes (the hydroclimate);

3. hydroregions correspond to the expression of hydrobelts on the different continents; they are contiguous.

The long-term objective of the hydrobelt delineation is (i) to facilitate the *Earth system analysis* related to riverine fluxes, land – ocean interactions, climate change impacts on river basins, past climate changes and (ii) to provide an *integrated analysis of water-related issues*, such as river changes, demographic trajectories and water resources analysis, for fixed spatial entities. Therefore, hydrobelts and hydroregions should also take into account the continental limits. Although hydrobelt delineation is designed to minimise intra-belt hydroclimate heterogeneity and to maximise inter-belt discrepancy, this optimisation was not conducted automatically by using purely quantitative criteria for the basin clustering. We also took into account previous studies of river basins at a global scale.

We focus on the non-glaciated part of continents, excluding Greenland and Antarctica. As they have few flowing rivers, they could only be considered in global tabulations as glaciated hydrobelts. The first level of aggregation defined eight hydrobelts based on the average annual temperature and run-off in the aggregated river basins (see Table 1 for the temperature and run-off targets):

– *Boreal belt* (BOR), essentially defined by its annual average temperature, below 0 °C, and only found in the Northern Hemisphere;

– *North and south mid-latitude belts* (NML and SML), defined by medium run-off and temperature figures and by their general latitudinal position centred at 45° N and 45° S;

– *North and south subtropical belts* (NST and SST), defined by an average temperature exceeding 15 °C, by medium run-off and by their position at 17° N and 17° S;

– *North and south dry belts* (NDR and SDR), only defined by their low run-off ($0 < q < 150\,\mathrm{mm\,yr^{-1}}$);

– *Equatorial belt* (EQT), defined by its high and relatively constant temperature throughout the year (annual average temperature $T > 20\,^{\circ}\mathrm{C}$) and its elevated run-off ($q > 750\,\mathrm{mm\,yr^{-1}}$), and by its position centred near the equator.

All of the belts have been named based on their latitudinal position, except for the dry belts, which have considerable latitudinal ranges (see below). The second level of aggregation of river basins is the decomposition of hydrobelts into hydroregions on each continent. Six continents are considered: North and South America; Europe including Anatolia; Asia separated from Europe by the Ural and South Caucasus Mountains and also including New Guinea; and finally Australia including New Zealand.

2.2 Datasets used to characterise the hydrobelts and hydroregions

The datasets used to divide and characterise the hydrobelts are detailed in Table 2 and fully tabulated in the Supplement. Two main hydroclimate indicators were used to delineate the hydrobelts: (i) the annual water run-off (q, $\mathrm{mm\,yr^{-1}}$), derived from the run-off data constructed at 30′ by Fekete et al. (2002). The dataset is based on a hydrological model that is calibrated against observed discharge, mainly for the period of 1960–1990. The run-off dataset we used does not take into account the impact of simulated water use, water withdrawal, nor dam construction (Fekete et al., 2002); and (ii) the average air temperature, available at a finer spatial resolution of 30″ (30 arc seconds; around 1 km at the equator) (Hijmans et al., 2005). Temperature data were aggregated

Table 2. Datasets used for the hydrobelt delineation and analysis.

Indicator/Index	Year	Source	Data format	Notes
COSCAT	~ 1960–1990	Meybeck et al. (2006)	Gridded Polygon	Global spatial data with 30′ resolution (~ 50 km at the equator)
Temperature	1960–1990	WorldClim v1.4 (Hijmans et al., 2005)	Raster	Global spatial data with 30″ resolution (~ 1 km at the equator)
Run-off	~ 1960–1990	Fekete et al. (2002)	Raster	Global spatial data with 30′ resolution (~ 50 km at the equator)
Precipitation	1960–1990	WorldClim v1.4 (Hijmans et al., 2005)	Raster	Global spatial data with 30″ resolution (~ 1 km at the equator)
Exorheism/endorheism	~ 1960–1990	Vörösmarty et al. (2000a, b)	Gridded Polygon	Global spatial data with 30′ resolution (~ 50 km at the equator)
Permafrost	~ 1960–1990	Brown et al. (1998)	Raster	Spatial data with 30′ resolution (~ 50 km at the equator); Northern Hemisphere only (very minor occurrences in the Southern Hemisphere)
Glacier cover	Quaternary	Dürr et al. (2005)	Polygon	Global data; maximum ice extent throughout one of the Quaternary ice ages (mostly Late Glacial Maximum, but not necessarily)
Holdridge life zones	1990	Leemans (1992)	Grid	Global spatial data with 5′ resolution (~ 10 km at the equator)
Climate regions	1975–2005	Rubel and Kottek (2010)	Polygon	The average Köppen–Geiger climate classification for the year 1975–2005
Population density	2005	HYDE (Klein Goldewijk et al., 2010)	Raster	Global spatial data with 5′ resolution (~ 10 km at the equator)

to a spatial resolution of 30′, similar to run-off data. The climate and hydrological data represent the situation in the latter half of the 20th century (in most cases 1960–1990). For our analysis the hydrological data (precipitation, run-off) were area weighted (discharge x area calculated per individual cell, then summed up per entity, and finally divided by total entity area).

Arheic areas are operationally defined here by an interannual run-off of less than $3\,\mathrm{mm\,yr^{-1}}$ (Vörösmarty et al., 2000a, b), based on the global hydrological model provided by Fekete et al. (2002). This limit between *arheism* (total absence of river flow) and rheism (some river flow, at least one flood event every 10 yr) has been verified for extremely arid regions, such as the Lake Eyre basin in Central Australia (Kotwicki, 1986).

The maximum Quaternary glacial extent is derived from the global-scale maps of Gerasimov et al. (1964) and other sources, digitised by Dürr (2003); according to Gerasimov et al. (1964) it mostly corresponds to the Late Glacial Maximum. We also took into account the classical descriptions made by hydrologists (Rodier, 1964; Korzoun et al., 1978; Haines et al., 1988). The geological history of river basins is derived from Potter (1978) and Potter and Hamblin (2006).

Hydrobelts are also compared to previous global analysis of the climate and vegetation on different continents done by Köppen (1931) and Holdridge (1967). The fish biodiversity description that we provide is adapted from Tedesco et al. (2008) and Abell et al. (2008). The ecozones description is from Schultz (2005).

The population data (Klein Goldewijk et al., 2010) is for the year 2005. Average population density is the ratio between the total population and the total area of any belt or region. Full ranges of cell attributes and latitudes correspond to the 5–95 % percentiles of their spatial distributions. A preliminary analysis of main human pressures is also presented, based on various regional to global-scale analyses (Meybeck and Helmer, 1989; Meybeck, 2003; Nilsson et al., 2005; Salomons et al., 2005; Vörösmarty, 2005, 2010; Seitzinger et al., 2010).

2.3 Delineation of hydrobelts

Delineating the hydrobelts was a stepwise, standardised process that considered the aggregation of river basins. First exorheic and endorheic river basins were separated. The *exorheic* drainage of the continents, i.e. connected to the world's oceans, includes 6140 river basins exceeding $400\,\mathrm{km^2}$ (catchment area ranging from $400\,\mathrm{km^2}$ to $6.1\,\mathrm{M\,km^2}$) at a resolution of 30′ (Vörösmarty et al., 2000a, b). The 47 largest river basins (exceeding $0.5\,\mathrm{M\,km^2}$) correspond to over half of the exorheic continental area (Meybeck and Ragu, 1995; Vörösmarty et al., 2000a, b; Milliman and Farnsworth, 2011). Therefore, the greatest parts of the belt boundaries correspond to these large basins, among which the Amazon (#1, $6.1\,\mathrm{M\,km^2}$), the Congo (#2, $3.7\,\mathrm{M\,km^2}$), the Ob (#3, $3.0\,\mathrm{M\,km^2}$), the Mississippi (#4, $3.0\,\mathrm{M\,km^2}$) and the Nile (#5, $2.9\,\mathrm{M\,km^2}$) are the largest ones. The next largest exorheic river basins ($n = 150$) were then considered. The remaining smaller basins ($n = 6000$) were finally clustered using a previous aggregation of world rivers into 156 coastal river catchment entities termed COSCATs (Meybeck et al., 2006).

COSCATs (median size of $0.45\,\mathrm{M\,km^2}$) were originally designed to harmonise the reporting of river fluxes to oceans at a global scale (Meybeck et al., 2006). They are continuous spatial entities delineated by river basin boundaries at the 30′ resolution. They originally were defined in two steps. First, two coastal cells used as boundaries were determined with multiple criteria as ocean floor topography, regional sea basin limits, continental limits, or a coastal run-off gradient. Then the COSCAT basin delineation is realised upland from the two boundary cells on the basis of the upstream river network (see detailed presentation of COSCATs in Supplement).

Since the *endorheic* drainage of the continents was not originally part of the COSCATs, the dataset was completed here by 91 additional endorheic river basins (median size of $0.086\,\mathrm{M\,km^2}$). The endorheic basins include the Great Basin (USA), the Caspian Sea basin, split between Europe and Asia, the Lake Chad basin, the Rift Valley and the Okavango River basin in Africa, the Aral Sea basin in Asia, the Lake Eyre basin in Australia and many smaller ones in Central

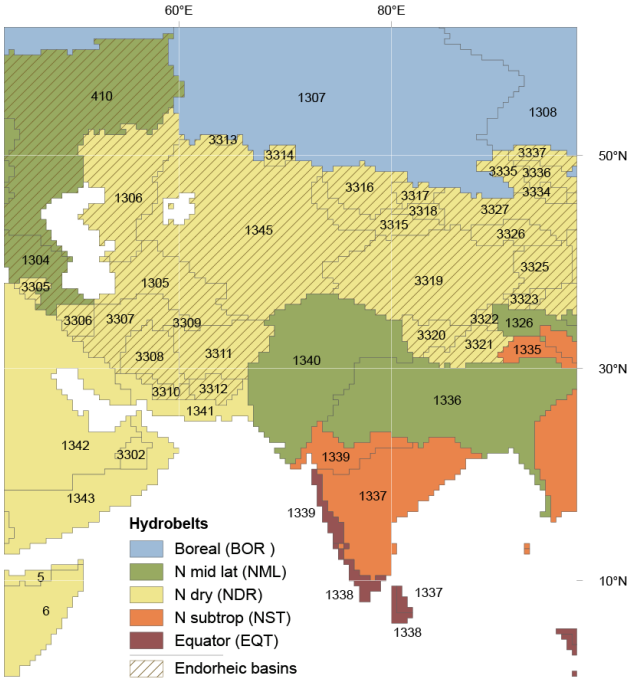

Fig. 1. Delineation of coastal catchments (COSCATs), exorheic and endorheic river basins and their aggregation into hydrobelts: example of Central and South Asia. COSCATs coding (except endorheic regions) from Meybeck et al. (2006) (see Supplement for tabulated information and coding of the endorheic COSCATs).

Asia, Australia and the Americas. All endorheic basins can be found in the dry belts, except the Volga Basin and the NW Caspian tributaries that have a medium to high run-off.

We needed to make several minor modifications to the original COSCAT division when delineating the hydrobelts. The modifications concerned first those islands and archipelagos which are originally attributed to several COSCATs due to the topography of the ocean floor and have now been re-attributed to single hydrobelts. A second set of adjustments concerned a few COSCATs that originally had mixed climate features, which we now split into two different hydrobelts (see details about these re-attributions in the Supplement).

The re-aggregation of the world's river basins results in a definition for 246 hydrological entities; these entities are limited by the natural drainage area limits. An example of how we delineated the COSCATs and their re-aggregation for Central and South Asia is schematically presented in Fig. 1. For instance, three adjacent cells in Tibet are linked, through river networks, to three receiving cells in the following ways: (i) the Indian Ocean through the Indus River; (ii) the Aral Sea through the Amu Darya River; and (iii) the Lop Nor salt lake in China through the Tarim River at its maximum extension.

Finally, we clustered these 246 entities into eight belts (see Fig. 2) until the intra-belt hydroclimatic homogeneity and inter-belt discrepancy could not progress any more without significantly fragmenting the belts into a number of pieces, thereby violating a major criterion (see Sect. 2.1). We also considered in this step former global outlooks on river basins made by physical geographers, particularly for endorheic basins, past glacial cover and river run-off regimes. This process was iterative and included multiple verifications and decisions regarding the identification and clustering of various hydrological conditions. The mid-latitude belt in Asia and the subtropical belts were the most difficult ones to define (see Sect. 3.2).

The hydroregions correspond to the portion of the hydrobelts present on each continent. In Asia the very large boreal (14.5 M km^2) and dry (13.6 M km^2) hydroregions present marked temperature differences and were split into two parts. The Asian boreal region (14.5 M km^2) was split into *West Siberia*, which faces the Arctic Ocean (BOR-Asi(WSb), 6.5 M km^2, −4.3 °C on average), and *East Siberia*, which faces the Arctic Ocean, the Bering Sea and the Okhotsk Sea (BOR-Asi(ESb), 8.0 M km^2, −9.7 °C on average). Similarly, the Asian northern dry region (13.6 M km^2) was split into the *Middle East*, which extends from the Jordan Basin to the Iranian endorheic regions (NDR-Asi(MdE), 5.2 M km^2, +21 °C),with only one major river, the Shatt El Arab (or Euphrates/Tigris), and *Central Asia* (NDR-Asi(CAs), 8.4 M km^2, +5.1 °C), which extends from the Eastern tributaries of the Caspian Sea to the Kerulen in Mongolia, including such Afghanistan rivers as the Helmand (Fig. 2). *All rivers of Central Asia, as defined here, are endorheic*. This contrasts with the Middle East rivers basins, of which only 23 % are endorheic; the Arabian Peninsula is presently arheic.

With these separations we were able to define 26 major hydroregions (see map in Fig. 2). Once we had delineated the belts and hydroregions, we used existing databases to establish their general attributes based on their cell distribution (median values and percentiles) and their cell area weighted averages.

3 Hydrobelts and hydroregions characteristics

In this section we present the hydrophysical characteristics of the hydrobelts, then the limitations of their delineation and their climate and vegetation characteristics. Finally, the hydrophysical characteristics of each hydroregion are briefly given.

3.1 General hydrophysical characteristics of hydrobelts

The general geographic position, size, the current proportions of the endorheic area, permafrost and past glacial cover (maximum Quaternary glacier extent – mostly Late Glacial Maximum (LGM)) for each belt are presented in Table 3, along with their average temperature, precipitation, run-off

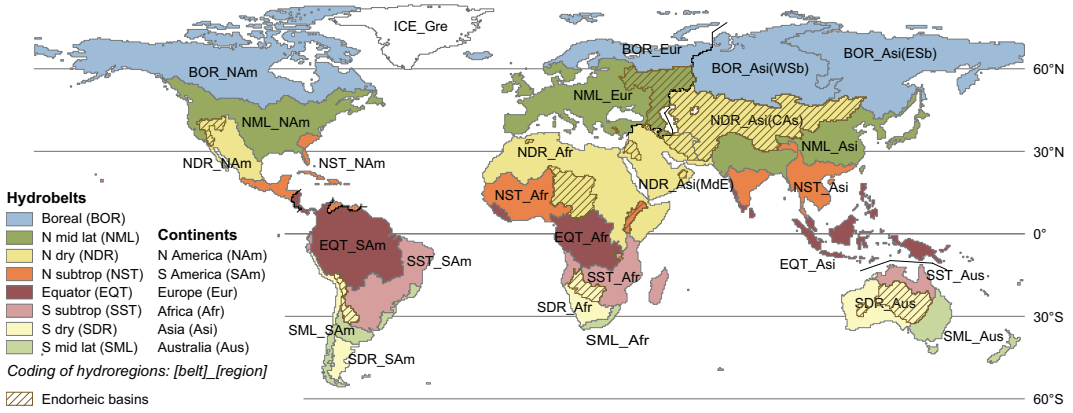

Fig. 2. Limits and coding of global hydrobelts and hydroregions.

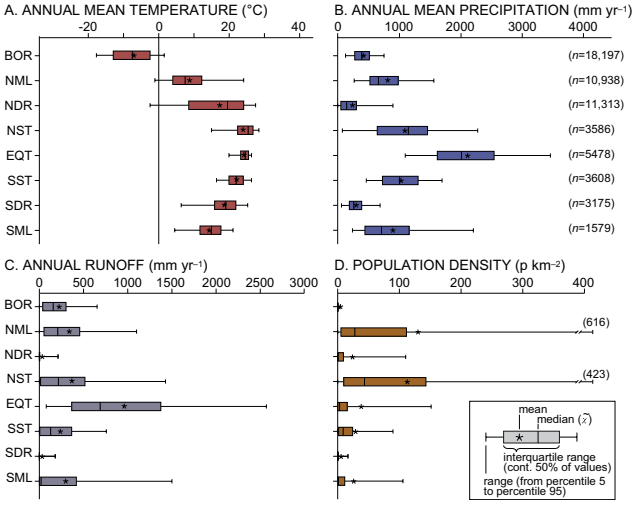

Fig. 3. Distribution of average annual cell characteristics in hydrobelts presented with box plot graphs. **(a)** annual mean temperature; **(b)** annual mean precipitation; **(c)** annual run-off; and **(d)** population density. BOR = boreal, NML = northern mid-latitude, NDR = northern dry, NST = northern subtropical, EQT = equatorial belts and SML, SDR, SST their southern analogues (see Fig. 2 for their spatial distributions). Ranges correspond to the 5–95 percentile distribution. Note: outliers are not plotted.

and population density (see also Fig. 3). The characteristics of each belt are introduced below along with their major rivers (see Supplement for a full list of river basins), river hydrological and thermal regimes, past Holocene history and sensitivity to climate change.

The *boreal belt* (surface area: 26 M km^2, mean elevation: 410 m) is the coldest of all belts. Its annual temperature is largely negative with −6.6 °C on average (ranging from −9.7 °C for East Siberia to −1.4 °C for Northern Europe; Table 4, Fig. 4). Its average latitude is 62° N, ranging from 49.7° N to 73.2° N (5 % to 95 % of the cell distribution). It extends throughout the northern parts of Europe, Asia and North America. The average precipitation (P) in the boreal belt is 437 mm yr^{-1}, resulting in an average run-off (q) of 223 mm yr^{-1} (Table 3).

Some of the world's greatest river basins are found in this belt. These include the Yukon, Mackenzie, Churchill and Nelson rivers in North America, the Northern Dvina and Pechora rivers in Europe, and the Ob, Yenisei, Lena, Indigirka, Kolyma, Anadyr, Penzhina and Amur rivers in Siberia. All of these rivers have sufficient run-off to reach the Arctic Ocean and regional seas (the Bering Sea and Sea of Okhotsk for the Pacific Ocean, and Hudson Bay and Ungawa Bay for the Atlantic Ocean). These rivers are frozen during several months of the year and are characterised by snowmelt river regimes with marked seasonal variations in run-off. This regime is characterised by a very pronounced late spring or early summer flood pulse, with ice jams that have huge erosive power on riverbanks (Costard et al., 2007), limiting the aquatic biota.

During at least one of the Quaternary ice ages, 54.3 % of this belt was covered by ice caps or glaciers (23 % in West Siberia, 34.7 % in East Siberia, 77.7 % in Europe and 88 % in North America;). Therefore, many of today's river networks are very recent (Potter and Hamblin, 2006). The last glaciers melted about 6000 yr ago, leaving multiple legacies that still impact present morphology, land cover, hydrology and biodiversity of the river basins: (i) the occurrence of major lake provinces – Canadian and Scandinavian shields and Taymir peninsula – and large wetland provinces (Lehner and Döll, 2004); (ii) the permafrost dominance (from 30 % to 88 % of their area, average 75 %); (iii) the specific coastal topography, such as fjords and archipelagos, associated with a hard, rocky coast (Dürr et al., 2011). The aquatic biota diversity, e.g. the richness of fish species and endemism, is limited in these river basins, which often have a very short history compared to other rivers in the world (Abell et al., 2008).

Table 3. General average characteristics of hydrobelts (cell averages, weighted averages and totals). BOR = boreal, NML = northern mid-latitude, NDR = northern dry, NST = northern subtropical, EQT = equatorial belts and SML, SDR, SST their southern analogues (see Fig. 2 for their spatial distributions and Table 2 for data sources).

Name	Mid-lat.	Area	Pop.	p_{dens}	Temp	Prec	Run-off	% of total area			
	(°)	(10^3 km^2)	(10^6 p)	(p km^{-2})	(° C)	(mm yr^{-1})	(mm yr^{-1})	Endorheic	Arheic	Permafr.	Glaciat.
BOR	60.5	25 995	123	4.7	−6.6	437	223	–	0.4 %	74.8 %	54.3 %
NML	41.3	24 199	3300	136.4	9.1	809	343	8.7 %	1.0 %	6.1 %	27.8 %
NDR	27.7	30 234	740	24.5	17.2	253	36	41.2 %	38.8 %	6.1 %	4.0 %
NST	16.7	10 579	1252	118.4	23.9	1112	383	3.5 %	0.7 %	1.7 %	1.7 %
EQT	−2.5	16 826	638	37.9	23.9	2124	960	–	0.2 %	–	–
SST	−16.9	10 599	303	28.6	21.9	1035	233	0.6 %	3.9 %	–	0.4 %
SDR	−26.4	8677	42	4.8	18.3	318	31	42.4 %	56.7 %	–	4.0 %
SML	−33.6	4008	109	27.3	14.5	872	292	–	4.7 %	–	10.7 %
Total*	31	131 119	6509	49.6	12.7	789	277	14.2 %	13.5 %	17.6 %	17.7 %

* Total of non-glaciated land.

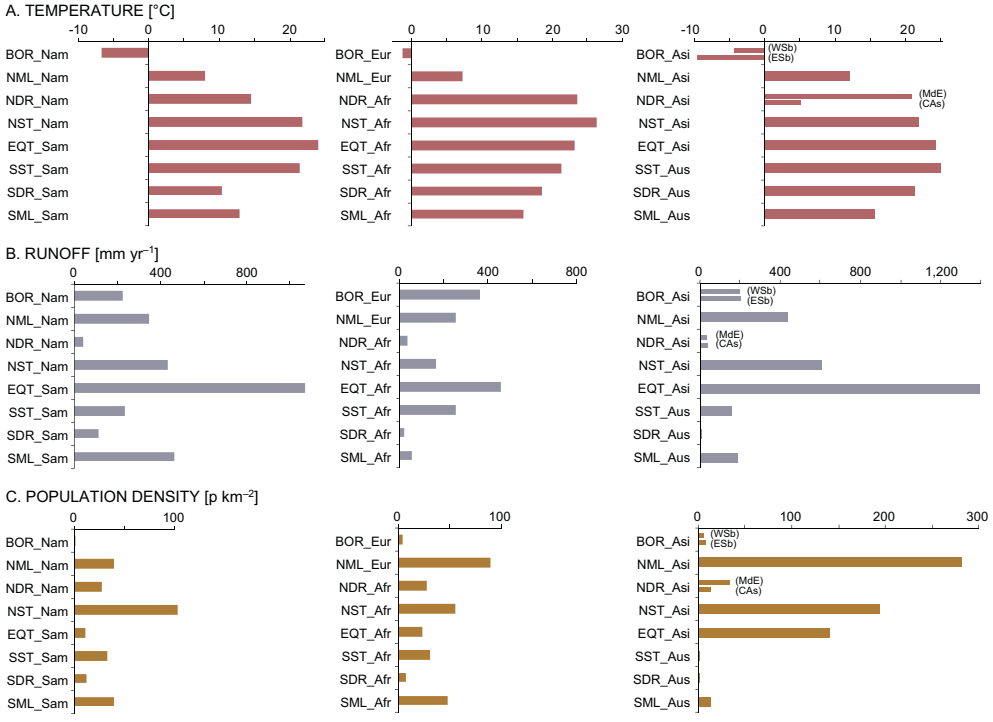

Fig. 4. North to south distributions for the 26 individual hydroregions on each continent along three north–south profiles: (1) North America (NAm) and South America (SAm), (2) Europe (Eur) and Africa (Afr), (3) Asia (Asi) and Australia (Aus). **(a)**: average temperature; **(b)**: run-off; and **(c)**: population density. BOR = boreal, NML = northern mid-latitude, NDR = northern dry, NST = northern subtropical, EQT = equatorial belts and SML, SDR, SST their southern analogues (see Fig. 2 for their spatial distributions).

3.1.1 Mid-latitude belts

Mid-latitude belts are characterised by their median run-off, close to the world average for exorheic regions, and their average temperature. Former glacial cover has affected them much less than the boreal hydrobelt. They have limited endorheic or arheic areas (Table 3). Due to the imbalanced distribution of land area between the Northern and Southern Hemisphere, the corresponding areas of the mid-latitude belts are quite different (24.2 M km^2 for the Northern Hemisphere vs. 4 M km^2 for the Southern Hemisphere) and their mean latitudes are somewhat different (43° N and 34° S). Mid-latitude river basins have contrasted thermal regimes and medium run-off seasonality, often regulated by snowmelt from mountain regions. A significant proportion of these

Table 4. General average characteristics of hydroregions (area weighted averages and totals) presented in three north–south profiles. BOR = boreal, NML = northern mid-latitude, NDR = northern dry, NST = northern subtropical, EQT = equatorial belts and SML, SDR, SST their southern analogues; North America (NAm), South America (SAm), Europe (Eur), Africa (Afr), Asia (Asi) and Australia (Aus). RPI stands for relative pressure indicator = (d_{pop}/q) hydroregion/(d_{pop}/q) N. Am boreal region. See Fig. 2 for the spatial distribution of hydroregions and Table 2 for data sources (see Sect. 4.2).

Name	Mid-lat.	Area	Pop.	p_{dens}	RPI	Temp	Prec	Run-off	% of total area	
	(°)	(10^3 km^2)	(10^6 p)	(p km^{-2})	(–)	(°C)	(mm yr^{-1})	(mm yr^{-1})	Endorheic	Arheic
BOR_Nam	60.6	9383	7.4	0.8	1	−6.7	426	224	–	1.1 %
NML_Nam	42.1	7667	304	39.6	33	8.0	874	345	–	1.2 %
NDR_Nam	31.2	2835	78	27.2	181	14.6	431	42	15.1 %	12.5 %
NST_Nam	19.7	1634	166	102.7	67	21.9	1441	434	–	1.7 %
EQT_Sam	−3.8	9183	100	10.9	3	24.1	2,171	1069	–	0.1 %
SST_Sam	−18.4	5054	169	33.4	40	21.5	1126	235	–	0.2 %
SDR_Sam	−31.5	1835	22	12.1	31	10.3	290	111	29.3 %	22.3 %
SML_Sam	−35.1	1696	66	39.1	24	12.9	1,031	462	–	0.3 %
BOR_Eur	65.2	2070	10	4.7	4	−1.4	608	364	–	–
NML_Eur	49.1	8633	778	90.0	101	7.2	660	252	24.4 %	0.5 %
NDR_Afr	18.7	13 825	382	27.6	223	23.6	290	35	17.9 %	51.6 %
NST_Afr	12.8	4704	260	55.2	95	26.3	735	165	7.8 %	0.8 %
EQT_Afr	−1.5	4620	111	24.1	15	23.2	1630	460	–	–
SST_Afr	−15.1	4230	134	31.6	35	21.3	966	254	1.6 %	2.4 %
SDR_Afr	−23.8	2150	16	7.4	114	18.6	390	18	39.9 %	16.1 %
SML_Afr	−31.0	387	19	48.3	244	15.9	616	56	–	34.3 %
BOR_Asi(WSb)	58.7	6529	38	5.8	8	−4.3	432	199	–	0.0 %
BOR_Asi(ESb)	60.6	8014	68	8.5	12	−9.7	409	206	–	0.1 %
NML_Asi	32.1	7900	2218	280.8	181	12.2	909	440	–	1.4 %
NDR_Asi(MdE)	27.0	5189	175	33.7	269	21.0	154	35	22.7 %	35.5 %
NDR_Asi(CAs)	41.6	8386	112	13.3	105	5.1	192	36	100.0 %	17.5 %
NST_Asi	19.9	4241	822	193.8	91	21.9	1,403	606	–	0.2 %
EQT_Asi	−0.1	3023	427	141.2	29	24.3	2738	1393	–	0.5 %
SST_Aus	−16.9	1314	0.9	0.7	1	25.1	908	157	–	22.7 %
SDR_Aus	−25.6	4692	3.9	0.8	42	21.3	296	6	48.6 %	88.6 %
SML_Aus	−32.7	1925	24	12.7	19	15.6	784	188	–	2.6 %
Total	31	131 119	6509	49.6	51	12.7	789	277	14.2 %	13.5 %

basins has been glaciated (27.8 % in the north, 10.7 % in the south).

The *northern mid-latitude belt* (24.2 M km^2, 761 m) is quite extensive. It is characterised by a medium positive temperature (mean hydroregions temperature ranging from +7.2 °C to +12.2 °C, +9.1 °C on average), precipitation (809 mm yr^{-1}) and run-off (343 mm yr^{-1}) – all of which are close to the world's means for the non-glaciated regions and non-endorheic regions (12.9 °C, 869 mm yr^{-1} and 340 mm yr^{-1}, respectively) (Tables 3, 4; Fig. 3). This belt ranges from a latitude of 26.7° N to 58.2° N (mean 41.3° N) and also extends throughout half of North America, more than 95 % of the European continent, large parts of Eastern Asia, and parts of Southern Asia. It is important to note that the NML belt is totally interrupted between Europe and Asia by the northern dry belt (Fig. 2) and fragmented in Asia into two parts, south and east of the Tibetan Plateau (Fig. 2).

These river basins of this belt are connected to the coastal ocean: the Columbia, Mississippi/Missouri and Saint Lawrence rivers for North America; the Rhine, Elbe, Rhone, Danube, Don and Dnepr rivers for Europe; and, the Indus, Ganges–Brahmaputra–Meghna, Yangtze (Chang Jiang) and Yellow (Huang He) rivers for Asia. This belt also includes the western Caspian tributaries from the Volga to the Kura, which are *sensu stricto* endorheic basins but characterised by medium to high run-off figures: this inclusion results in an exceptional endorheism rate of 8.7 % for this belt.

In mountain ranges many of these NML basins were exposed to glacial cover (27.8 % on average), and the legacies of the glaciations can be important: 14 % of the basin area in Asia, 25 % of those in Europe and 44 % of those in North America. This rate reaches 100 % for the Saint Lawrence River basin (attributed to this belt based on its latitudinal position). In comparison, the Danube River basin has been

much less glaciated. The extent of the present permafrost is also limited in the NML belt, compared to the boreal belt (6.1 % vs. 74.8 %).

Rivers of the NML often have their headwaters in colder climate areas (Rocky Mountains, Alps, Caucasus, Central Asia, and Himalayas), resulting in marked longitudinal gradients of temperature and hydrological regimes, mixing snowmelt and/or icemelt in the headwaters of the rivers, and rainfall-evaporation dominance in the lower tributaries. Such contrasts are at their maximum in Asia and made the belt delineation delicate (see Sect. 3.2). The river ecology of the mid-latitude regions can also be complex and it varies spatially, reflecting the longitudinal variations (e.g. Tedesco et al., 2008). The fish population diversity of the related hydroecoregions is intermediate between those of the boreal rivers and the subtropical and equatorial rivers, with the exception of the Asian hydroregion (Abell et al., 2008).

The *southern mid-latitude belt* (4.0 M km^2, 507 m) is different from its northern analogue in many ways. It is six times smaller (4.0 M km^2 versus 24.2 M km^2) and much warmer (+14.5 °C versus +9.1 °C). Its main hydroclimate characteristics are, nevertheless, similar in terms of precipitation (862 mm yr^{-1} versus 809 mm yr^{-1} for NML) and run-off (292 mm yr^{-1} vs. 343 mm yr^{-1}) (Table 3; Fig. 3). The temperature difference between the north and south mid-latitude belts is mostly due to the continentality of the NML since their mean elevation is relatively close (761 m vs. 507 m). This belt is essentially exorheic and it can be found on three continents: it covers the westward tip of South America, along the coast of Chile and in central Argentina, a narrow strip of coastal basins in southeast Africa, and is found in eastern Australia (Murray–Darling River basin) and in New Zealand. As the continental climate is totally absent in this belt (see Sect. 3.3), the thermal and hydrological regimes of these rivers are different from those of the northern mid-latitude belt: the influence of snowmelt is very limited, except in parts of New Zealand and Patagonia (Haines et al., 1988).

3.1.2 Dry belts

The northern and southern dry belts are characterised by common hydrological features: (i) high proportions of endorheism (41 % of the total area) and/or arheism (43 %), (ii) allogenic rivers, (iii) waddis, and (iv) a high sensitivity to climate variations. The proportion of endorheic basins in the dry hydroregions ranges from 15.1 % in North/Central America to 100 % in Central Asia (Table 4). Dry hydroregions have generally not been formerly glaciated, except for South America (18.8 % of basin areas) and Central Asia (3.7 %) (Table 4).

Allogenic rivers are quite representative of the dry belts basins, although not exclusively located there. Allogenic rivers correspond to river regimes controlled by headwater hydroclimate: snow- and icemelt as in Central Asia (Amu Darya, Syr Darya, Tarim rivers), higher rainfall (Nile, Chari, Orange rivers), or their combination as in North America (Colorado and Rio Grande rivers). These more humid headwaters, with local positive water balance, are generally located in high-relief regions while the rest of their basin is located in semi-arid or arid lowlands, with local negative water balance: they correspond to water towers, as defined by Viviroli et al. (2007). Other allogenic rivers (e.g. Niger, Indus, Huang He, Murray rivers) correspond to those basins, which have been difficult to attribute to a given hydrobelt (see Discussion). Water towers are essential features of the dry belts, but they may also be observed in more humid mountain basins of the mid-latitude belts originating from the Rocky Mountains, Alps, Caucasus, Andes, and even in Alaska (Viviroli et al., 2007).

When the water balance of the allogenic river basins is positive, they naturally fill the land depressions and reach the coastal ocean. If not, they constitute endorheic basins where the totality of the water generated in the water towers is ultimately evaporated via salt pans (Uyuni, Lop Nor, Kara Bogaz), saline aquifers (Lake Chad) and internal brackish (Caspian Sea, Aral Sea, Balkash Lake) or hypersaline lakes (Dead Sea, Great Salt Lake). Therefore, allogenic rivers of the dry belt can be either exorheic or endorheic (*): the Colorado, Rio Grande/Bravo, Pampa rivers, Chari/Logone (*), Nile, Orange, Shatt el Arab, Amu Darya (*), Syr Darya (*), Tarim (*), Kerulen (*), Murray. The Indus and Huang He rivers, also allogenic, are attributed to the mid-latitude belt (see discussion). Regular annual hydrographs are observed for allogenic rivers fed by water towers, such as the Nile, and/or for fed by snow- and icemelt as in Central Asia (e.g. Shatt el Arab, Amu Darya, Syr Darya, Tarim) (Dukhovny and De Schutter, 2011). All allogenic rivers are very sensitive to their water tower climate, for precipitation changes and/or for temperature changes (Viviroli et al., 2007).

Waddis are generally lacking humid headwaters and are highly irregular rivers characterised by flash floods, marked seasonal dryness, and large inter-annual variations. In the very dry and/or smallest basins these rivers may not flow at all for a year or more (q between 3 mm yr^{-1} and 30 mm yr^{-1}), as in the Lake Eyre basin (Kotwicki, 1986). During the rare flow events, the specific run-off in waddis can exceed 1000 L km^{-2} s^{-1}, with catastrophic flooding and enormous sediment transport, which are seldom described in the scientific literature (Cruette and Rodier, 1971; Milliman and Farnsworth, 2011). Water resources in waddis are therefore very difficult to store and manage, in contrast to most allogenic rivers basins.

Dry belts are very sensitive to climate variations, particularly for precipitation and run-off, as shown by palaeohydrological studies, which still need to be synthesised on a global scale. When the climate becomes drier, the permanent flows (typically more than 100 mm yr^{-1} run-off) are first turned into highly seasonal flows (30 to 100 mm yr^{-1}), typical of

allogenic permanent rivers, then into non-permanent flows (3 to 30 mm yr^{-1}), resulting in seasonal dryness and river course fragmentation that characterises waddis. Finally, the changing climate may lead to permanent dryness or arheism (< 3 mm yr^{-1}) and filling by aeolian deposits. Such a trajectory is the one that has been observed, for example, for the Sahara and Arabia River networks over the last 6000 yr: the lower Nile tributaries were active, Lake Turkana was connected to the White Nile (Nyamweru, 1989), and the Sahara mountain massifs – Hoggar and Tibesti – served as the headwaters for numerous past allogenic rivers (Sarnthein et al., 1980; Said, 1993; Petit-Maire and Guo, 1995). Other examples are known from Asia (Caspian, Aral and Balkash lake connections, Kerulen to Amur connection), the Americas (Great Salt Lake basin connected to Columbia River basin, Mar Chiquita basin connected to Paraná) and Central Australia (Fairbridge, 1972; Dukhovny and De Schutter, 2011).

The *northern dry belt* (30.2 M km^2, 938 m) has the greatest surface area of all belts. It corresponds to catchments with very low run-off (average 36 mm yr^{-1}), which is almost ten times lower than the global average for exorheic rivers. It covers a wide latitudinal range, from 6.7° N to 47.7° N (mean 27.7° N) and a large elevation range, with elevation maximum in Central Asia (Table 3). This results in marked differences in average annual temperatures which range from +5 °C to +24 °C between hydroregions (Table 4; Fig. 4). The belt can be found on three continents: (i) in North America (Colorado and Rio Grande/Rio Bravo basins, both exorheic); (ii) in Northern Africa, where it includes the Sahara Desert from the Mauritanian coast to the Red Sea plus the endorheic Lake Chad basin; and (iii) in Asia, from the Arabic Peninsula and the East Caspian basins to Mongolia, including only one major exorheic river basin, the Shatt el Arab (or Euphrates/Tigris), and numerous endorheic ones (Ural, Tedzhen, Helmand, Amu and Syr Darya, Balkash Lake basin, Dzungaria, Tarim, Kerulen).

The *southern dry belt* (8.7 M km^2, 789 m) extends from 17.2° S to 44.2° S (mean 26.4° S). Due to the landmass distribution, its area is less than one-third of that of its northern counterpart. Despite a higher precipitation average (318 mm yr^{-1} versus 253 mm yr^{-1}), the average run-off figures are equivalent ($q = 31$ mm yr^{-1} in the SDR versus 36 mm yr^{-1} in the NDR) (Table 3; Fig. 3). The southern dry belt is also largely characterised by endorheic basins (42.4 %) and arheic areas (56.7 %). It is more fragmented than its northern counterpart. In South America, the belt is split into four parts: the exorheic, but very dry, Peruvian coast; the endorheic Altiplano Plateau (Titicaca Lake basin); the endorheic Mar Chiquita basin; and the exorheic Argentinean Pampa, which is fed by numerous allogenic rivers. In Southern Africa, it corresponds to the endorheic basins of the Etosha Pan and the Okavango swamps and to the large Orange River allogenic basin. In Australia this belt is particularly developed, including the huge endorheic Lake Eyre basin (1.17 M km^2) and numerous smaller endorheic and/or arheic basins in Central and Western Australia.

3.1.3 Subtropical belts

The northern and southern subtropical belts have the following hydrological features in common: (i) an even thermal regime with warm conditions throughout the year, with an average annual temperature ranging from 21.3 °C to 26.3 °C; (ii) marked seasonal precipitation regimes, e.g. the West African and Asian-Australian monsoons; (iii) marked seasonal run-off regimes. In such a river regime, the ratios of maximum over minimum monthly discharges may largely exceed a factor of ten in large basins (Rodier, 1964; Haines et al., 1988). The extent of floodplains and/or internal wetlands is also highly seasonal, creating some of the world's largest existing river wetlands, such as in the Paraná (Pantanal and Lower Paraná floodplain), the Niger (Delta Central) and the Mekong (Tonle Sap) rivers. Holocene river network variations may still be important in the driest portions of these belts in Africa and South America. They have not been influenced by past glaciations, and are essentially exorheic (96.5 % in NST and 99.4 % in SST): their geological history is long and relatively steady, compared to the boreal and dry belts. As a result, fish diversity in the subtropical rivers varies from medium to extremely high, as in the Asian subtropical hydroregion (Abell et al., 2008).

The *northern subtropical belt* (10.5 M km^2, 541 m) extends from latitude 7.2° N to latitude 25.2° N (mean 16.7° N). It is characterised by warm conditions throughout the year (+23.9 °C). In contrast, precipitation (1112 mm yr^{-1} annually on average), generated by the African and Asian monsoons, is seasonal, resulting in a medium amount of run-off (383 mm yr^{-1}) (Table 3; Fig. 3). This belt extends across Central America and the Caribbean Islands, from Florida to the coast of Columbia, across Africa, where it consists of two parts, separated by the northern dry belt, West Africa (the Niger Basin and the smaller basins of the Gulf of Guinea) and the northern East African Rift. In South Asia the NST belt is also split: the East Deccan dry evergreen forests (Cauwery to Godavari basins) are disjointed from the Southeast Asian basins from the Irrawaddy (Ayeyarwaddy) to the Pearl River (Zhu Jiang).

The *southern subtropical belt* (10.6 M km^2, 591 m) has an area similar to its northern analogue and extends from a latitude of 4.7° S to a latitude of 30.7° S (men 16.9° S). Its water balance ($P = 1035$ mm yr^{-1}, $q = 233$ mm yr^{-1}) and annual temperature (+ 21.9 °C) are also similar to those of the NST belt. The belt extends mostly through South America (5.5 M km^2) from the Sao Francisco to the Paraná basins and in the coastal basins of Ecuador (Fig. 2), in Southern Africa (4.23 M km^2) (Zambezi and Limpopo basins, and Madagascar), and in northern Australia (Flinders, Mitchell basins).

3.1.4 Equatorial belt

The *equatorial belt* (16.8 M km^2, 492 m) is unique and lies on both sides of the equator (14.2° S to 8.2° N). When delineated by basin boundaries, its mean latitude is slightly shifted to the south (2.5° S). It is very warm (+23.9 °C). The rainfall pattern is much less seasonal and wetter (2124 mm yr^{-1}) than in the subtropical belts, resulting in the maximum belt run-off (960 mm yr^{-1}) (Table 3; Fig. 3).

The belt is particularly developed in the South America hydroregion, from the Magdalena to the Tocantins rivers, where it includes two out of three of the world's greatest rivers in terms of discharge: the Amazon (#1, 6590 km^3 yr^{-1}) and the Orinoco (#3, 1135 km^3 yr^{-1}). In Africa it includes the Congo River (#2, 1200 km^3 yr^{-1}). These three rivers correspond to 60 % of the equatorial belt area and their enormous water discharge is responsible for approximately 20 % of the dissolved material inputs to oceans (Meybeck, 1988; Milliman and Farnsworth, 2011). In contrast to these three giant basins, in South and Southeast Asia this belt is very fragmented, corresponding to much smaller basins (< 100 000 km^2) located in narrow coastal strips (West Deccan, Sri Lanka) and on islands (Indonesia and the Philippines). These small- to medium-sized basins are characterised by some of the world's highest river run-off, exceeding 2000 mm yr^{-1} (e.g. Fly, Sepik, and Digul rivers in New Guinea).

Equatorial river basins have several features in common: (i) a high annual run-off, (ii) steady thermal and hydrological regimes with limited seasonal variations, and (iii) a very pronounced aquatic biodiversity. Their average run-off is 1393 mm yr^{-1} in Asia and 1069 mm yr^{-1} in South America, but only 460 mm yr^{-1} in Africa due to the Congo River basin, which cannot be fragmented (see the discussion in Sect. 3.2). The river regimes are regular with limited seasonality: their specific discharges at low flow rates are quite high compared to all other regions (Rodier, 1964; Haines et al., 1988). The Amazon and Congo hydrographs are – compared to the other big rivers of the world – very regular with limited seasonal variations (maximum to minimum monthly discharge ratio less than three for the Amazon and less than two for the Congo).

The Amazon, Orinoco and Congo River basins are among the oldest, millions of years old, and thus most stable in the world, in contrast to many other large rivers that have been either exposed to climate variations (e.g. Central Asia), influenced by active tectonics (South and SE Asia) or exposed to past ice cover (boreal belt) (Potter, 1978). The first two have marked altitudinal gradients and combine various biotopes (up to 13 hydro-ecoregions for the Amazon, according to Abell et al., 2008). The Congo River basin includes one of the world's biodiversity hotspots, Lake Tanganyika. These features may explain why their fish biodiversity is exceptional, with indicators more than ten times greater (Abell et al., 2008) than those observed for many boreal river basins of similar sizes, in which the present fish communities only began to develop 6000 yr ago.

This first analysis shows that the eight hydrobelts are well differentiated regarding their basin hydroclimate (temperature and run-off), their river hydrological or thermal regimes, the way in which they are connected with the oceans of the world (exorheism versus endorheism), their absence of flow (arheism), their past glacial history, and their sensitivity to precipitation changes. Although hydrobelts were designed to present the hydroclimate of continents in a symmetrical way, some important differences between the analogous northern and southern belts remain (Fig. 3 and Table 3). These differences combine (i) the uneven distribution of land masses (NML is, for example, colder than SML, implying also less evaporation and thus 15 % higher run-off) and the lack of a continental land mass south of 55° S, resulting in the absence of a boreal belt in the Southern Hemisphere; (ii) the occurrence of the continental climate only found in the northern belts. The mean elevation does not discriminate belts by much, but is very important when considering the hydroregion level.

3.2 Limitations of hydrobelt definitions

Ideally, hydrobelts should be very homogenous, delineated in one piece and very different from one another and defined by continental boundaries, as defined in our objectives. In reality, these objectives are subject to limitations, which are directly dependent on the first and third criteria (the delineation of river basins and continental boundaries).

3.2.1 Delineation sensitivity

One target of the delineation was to minimise the intra-belt hydroclimate heterogeneity based on temperature and run-off, and to maximise the inter-belt discrepancy. Some regions and/or basins have been on the edge of our attribution, either due to their natural heterogeneity (see below) or due to their geographic situation between belts. Also, we aimed at a minimum number of hydroregions, a certain north–south symmetry, and a balanced distribution of belts on the continents.

The most sensitive areas in our delineation were as follows:

- The Huang He (Yellow River; part of NML belt), which could also be part of the northern dry belt due to its low run-off. As an exorheic river we considered it, however, to be closer to the Yangtze than to the Tarim or Kerulen basins.

- The large Himalayan rivers, from Indus to Mekong, were difficult to attribute due to the natural heterogeneity of the basins. These basins extend from the polar to the dry climates (Indus basin; COSCAT #1336) or wet tropics (Ganges–Brahmaputra basin; COSCAT #1332). After a detailed hydroclimate analysis, we considered

both entities to be closer to the northern mid-latitude belt, while we attributed the Irrawaddy and Salween (Nu Jiang) basins (COSCAT #1331) and the Chao Phraya and Mekong (Lancang Jiang) basins (COSCAT #1325), with less extended upper valleys, to the subtropics.

- The Ethiopian Plateau was also difficult to split. The unity of the Nile basin had to be kept and the other basins (Awash and Omo basins, 0.37 M km^2) were attributed to the subtropical belt, based on their higher run-off (200 mm yr^{-1}).
- The southern mid-latitude hydroregions are not always well defined: they are fragmented in South America, limited to a small fringe in Africa, heterogeneous in Australia where the Murray–Darling river system, a typical allogenic river system with low run-off (less than 7 mm yr^{-1}), is mixed in the related hydroregion with much wetter New Zealand basins. The eastern tip of Southern Africa (0.4 M km^2) was attributed here to the southern mid-latitude belt, despite its relatively low run-off and high temperature (Fig. 4; Table 4), based on its river run-off regimes and to keep a balance between the continents. As such it is separated from the rest of the much drier and less-populated Southern Africa (Orange basin). However, this hydroregion is clearly an outlier when compared to the other mid-latitude regions (see Sect. 4.2; Fig. 4).

Considering our constraints and objectives, it can be estimated that such sensitive allocations to a given belt correspond to about 6 M km^2 out of 131 M km^2 of non-glaciated areas. Different aggregations would not much affect the overall hydrobelt characteristics but could matter at the hydroregion scale, particularly in Southern Asia, Australia or Southern Africa.

3.2.2 Fragmentation of hydrobelts and hydroregions cannot be avoided

Hydrobelts and hydroregions are limited by river basins and continental boundaries. We accepted one minor exception to this general rule: between Central America and the northern coast of South America, where two hydroregions overlap with one another (NST-Nam and EQT-Sam, Fig. 2). We decided that it was better to hold out the northern subtropical region around the Caribbean Sea basin. The fragmentation of some hydroregions results from the uneven distribution of relief and hydroclimates on continents (e.g. South American dry, African equatorial, Asian subtropical belts) and from the occurrence of islands (Asian equatorial belt).

Some hydroregions are not contiguous and could be split in further analyses into separate sub-regions, particularly from the population point of view. In Asia, mid-latitude hydroregion river basins from the Indian subcontinent can be separated from Chinese basins. In the African equatorial hydroregion (West African entity and Congo Basin) and in the South American dry region (Chile/Peru coast and Altiplano vs. Pampa), sub-regions can also be individualised.

3.2.3 Hydroclimate heterogeneity within a given belt cannot be totally reduced

The amount of hydroclimate heterogeneity in hydrobelts cannot be totally reduced for two reasons: (i) the use of river basin boundaries as a delineation rule: for example, the Congo River basin (3.7 M km^2) as a whole extends beyond the wet tropics and includes a large amount of drier steppes, as defined by Holdridge (circa 1 M km^2). As this heterogeneous basin could not be fragmented into different belts, it has been allocated to the African equatorial hydroregion, for its geographic situation. It has a much lower run-off (324 mm yr^{-1}) than the other part of the African equatorial belt, centred in Sierra Leone ($q = 1450$ mm yr^{-1}). Average run-off for the hydroregion is only 460 mm yr^{-1}, i.e. only half that of the other equatorial regions (Fig. 4b; Table 4); (ii) some elongated rivers oriented in a north to south direction cross different climate zones (e.g. the Nile, the Paraná River, many Siberian and Canadian rivers, and many South and Southeast Asian rivers); (iii) west–east gradients of precipitation and/or temperature, amplified by coastal mountain ranges, may induce marked heterogeneity in such basins (e.g. the Niger and Congo rivers); (iv) spatial climate variability can be quite high in mountainous areas controlled by present-day tectonics, as, for example, in the Ethiopian Rift Valley and in the Himalayas. All these factors may limit the homogeneity within large basins, hence within a given belt.

The temperature range within hydrobelts (5 to 95 % distribution of cell attributes) illustrates this residual heterogeneity (Fig. 3a–c). If the boreal belt is excluded, the intra-belt temperature ranges may exceed 25 °C for two northern belts (mid-latitude and dry), i.e. more than the inter-belt range of average temperatures (15 °C) (Fig. 3a). In contrast to the 5–95 % range, the interquartile ranges (25–75 %) for temperature, precipitation and run-off distributions better differentiate each hydrobelt (Fig. 3b and c, respectively).

3.3 Climate and vegetation distribution in hydrobelts

We aimed at maximising the homogeneity within the hydrobelts and the differences between them. As discussed before, this objective cannot be fully achieved and hydrobelt climate and vegetation types are not fully homogeneous.

The analysis of the five Köppen climate zones in hydrobelts is a good example of the limits of hydrobelt homogeneity (Fig. 5a). Four hydrobelts are well within a single dominant Köppen climate zone, i.e. exceeding 75 % of the belt area, while the other belts are situated within two main climate zones.

The seven Holdridge life zones are fragmented more often by hydrobelts partly because there are more life zones than climate zones. Most belts include two or three dominant

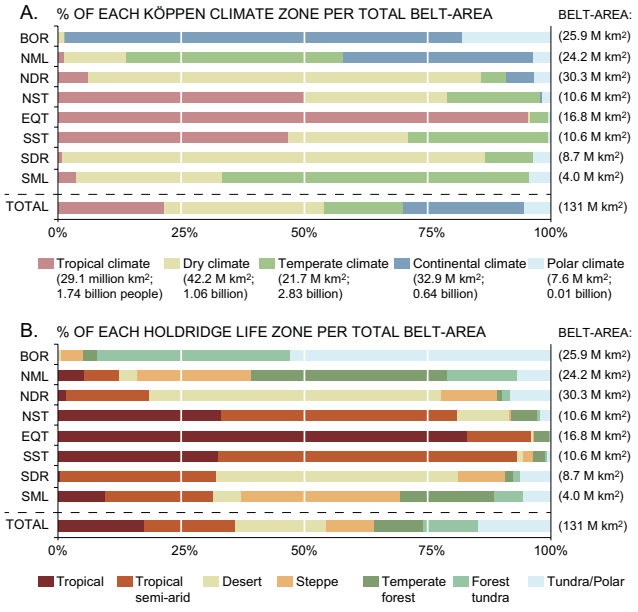

Fig. 5. Distribution of the proportions of Köppen climate zones **(a)** and of Holdridge life zones **(b)** in hydrobelts, in % of total for a given belt.

zones, except for the equatorial belt, which is found at 81.8 % within the Holdridge tropical zone (Fig. 5b). The boreal, equatorial and northern and southern dry belts are the most homogeneous belts, with only one clearly dominant type, while the mid-latitude and subtropical belts are the least homogeneous ones, combining two dominant climate types and three vegetation zones.

3.4 Hydroregions

Hydroregion characteristics are given in Table 4 and presented in Fig. 4 for annual mean temperature, run-off and population density for three north–south profiles for the Americas, Europe and Africa, as well as Asia and Australia. The temperature and run-off profiles are relatively similar and present a north–south symmetry, with the exception of the SML-Africa region (0.4 M km^2), which is warmer and drier than the SML hydroregions in South America and in Australia. The population density of hydroregions is controlled by the hydroclimate and by the uneven history of human settlement on the planet. This analysis is further developed in the following.

4 A first application of hydrobelts and hydroregion analysis: global population

In this section we first analyse the global population distribution at the hydrobelt level followed by the hydroregion level. We further explore the heterogeneity of the relation of population and water using a relative potential pressure index (RPI). Finally, we compare the population distribution at three spatial resolutions.

4.1 Population distribution in hydrobelts

The human population in hydrobelts is based on 2005 estimates (Klein Goldewijk et al., 2010), i.e. for a global population of 6500 million people (Tables 3, 4; Fig. 3d). As expected, the north and south hydrobelts differentiate the global distribution of population.

- The *boreal belt* is the least populated of all belts, with 123 Mp (million people). Only 1.9 % of the world's population lives in this cold area which covers 19.8 % of the planet's total area; it has quite low mean population densities, 4.7 p km^{-2}.
- The *northern mid-latitude belt* is the most heavily populated belt, with 3300 Mp; this represents 50.8 % of the total world population living on only 18.5 % of the non-glaciated continental landmass. Its average population density is 136 p km^{-2}.
- The *northern dry belt* holds 11.5 % of the world's population, despite very limited water resources. In these very dry to desert-type areas, which are present across a large temperature range, population densities (average 24.5 p km^{-2}) are still one order of magnitude higher than those found in the boreal regions.
- The *northern subtropical belt* is the second one in terms of total population, with a total of 1252 Mp (19.2 % of global population for 8.0 % of land). The mean population densities are high, 118 p km^{-2} on average, i.e. more than twice the average population density for the world.
- The *equatorial hydrobelt* is presently less populated than the world's average (37.9 p km^{-2} versus 49.6 p km^{-2}), totalling 638 Mp, i.e. 10 % of the world's population living on 12.8 % of the world's land area.
- The *southern subtropical belt*, not as extended as its northern counterpart, is four times less populated, with densities of 28.6 p km^{-2} (compared to 118.1 p km^{-2} for the north) and a total population of only 303 Mp.
- The *southern dry belt* has the smallest population of all belts, with only 42 Mp and a very low average density, 4.8 p km^{-2}, which is equivalent to that of the boreal belt and five times lower compared to the northern dry belt.
- The *southern mid-latitude belt* supports only 109 Mp, i.e. 30 times less than its northern analogue. This discrepancy is due to its small size and to its mean population density, 27.3 p km^{-2}, eight times lower than its northern counterpart and similar to that of the southern subtropical belt, 28.6 p km^{-2}.

As a result of these distributions, 81.4 % of the world's population lives in the three northern hydrobelts (northern mid-latitude, northern dry, northern subtropics), which cover 49.6 % of the non-glaciated continental landmass. The population density is five times greater in the northern belts than in their southern analogues (Table 3; Fig. 3d). Only 16.6 % of the population lives in the equatorial and southern belts, which cover 30 % of landmass, whereas 1.9 % of the world's population lives in the boreal belt, which covers 19.8 % of the planet's land area (Table 3).

In summary, *human population is not distributed on the continents according to the same statistical laws as the hydroclimate attributes* (Fig. 3d). The intra-belt range of population density, as measured by the 5 % to 95 % percentile ranges on 30′ cells, is greatest in the northern mid-latitude belt and the northern subtropical belt, i.e. in the most populated belts (an average of 136 and 118 p km^{-2}, respectively). This is probably due to the occurrence, and sometimes the dominance, of urban population hotspots. Further work is needed to confirm this hypothesis. Population density is mostly limited by hydroclimatic conditions in the boreal belt, and less so in the dry regions. This is supported by the findings of Kummu et al. (2011). The main control factors explaining the north versus south and "Old World" versus "New World" population discrepancies are linked to the different histories of human settlement (McNeill and McNeill, 2003; Klein Goldewijk et al., 2010), as we demonstrate in the following when hydroregion population is considered.

4.2 Population and human pressure in hydroregions

The population differences highlight the various hydroregions on each continent through the variability and relative importance of population and water run-off. To illustrate this global heterogeneity, we focus on the potential human pressure on surface waters at the hydroregion level, normalised to boreal regions, least populated with regards to the river run-off. This *relative potential pressure indicator (RPI)*:

$$\mathrm{RPI} = (d_{\mathrm{pop}}/q)\mathrm{hydroregion}/(d_{\mathrm{pop}}/q)\mathrm{N.\ Am\ Boreal}, \quad (1)$$

where d_{pop} stands for population density and q for run-off. RPI ranges from 1.0 (for the North American boreal hydroregion) to 269 (for the Middle East hydroregion). We use this indicator here to quantify and map the relation between population and run-off in each hydroregion (Table 4, Fig. 6). Water availability for population is typically a reverse indicator to RPI, i.e. expressed as m^3 capita^{-1} yr^{-1}, as established first by Falkenmark at the country level (Falkenmark and Lindh, 1974; Falkenmark et al., 1989), then used at a much finer resolution made possible by GIS analysis at resolutions such as 30′ (e.g. Arnell, 2004; Alcamo et al., 2007; Islam et al., 2007; Kummu et al., 2010). We consider that RPI provides an estimate of the overall pressure on river basins. In further studies the water resources availability and use of water resources, addressed at higher resolution, should be reported at the hydroregions level.

The spatial distribution of the potential human population pressure on river run-off by hydroregions (Fig. 6) illustrates the general north to south and Old World–New World disparities. The geometric progression of the indicator is validated on various global and regional water quality assessments (Meybeck and Helmer, 1989; Salomons et al., 2005). Only 8 regions are found in the blue ($1 < \mathrm{RPI} < 10$) and green domain ($10 < \mathrm{RPI} < 20$), where impacts are limited, 7 in the yellow domain ($20 < \mathrm{RPI} < 50$), 3 in the orange domain ($50 < \mathrm{RPI} < 100$) and 8 in the red domain ($\mathrm{RPI} > 100$). More than half of the world's population (3.7 billion) is living in the red zone, which covers now about 40 % of the global river basins (49 M km^2). On average, the potential pressure has already reached fifty times the pristine reference level established in northern Canada and Alaska.

Such global picture provides only a first-order analysis of human pressure on river basins. Each major river has its specific pressures and related trajectories (e.g. Meybeck, 2003). A more detailed analysis and discussion for each hydrobelt is given in the Supplement.

The following conclusions can be made: (i) differences between population densities for hydroregions of the same belts can exceed those noted between belts; (ii) for a given belt the following order is generally found, from the most to the least densely populated: Asia > Europe > North America ≥ Africa > South America ≫ Australia; (iii) the relative human pressure, i.e. the ratio of population density over annual run-off, normalised to its minimum figure in the North American boreal region, is a first-order indicator for overall human impact on river basins, although it is not always appropriate to measure impacts from dams, mining, or agriculture. It ranges over more than two orders of magnitude from 1 to 269 (Middle East) and is maximum in northern dry regions and in mid-latitude and subtropical Asia. The population distribution fully justifies consideration of each hydroregion as a distinct spatial entity when addressing human-related water issues.

4.3 Reporting scales of global water issues

Nowadays, global mapping can be done at high resolution, but the *reporting of results* is not yet harmonised: continental scale, political or economic regions, or country levels are commonly used. They are compared here, for the population distribution at the global scale, with three sets using natural river basin boundaries: hydrobelts, hydroregions, and coastal catchments. We represent the population of each entity by bubble charts within a temperature vs. run-off domain (log scale for run-off) (Fig. 7).

At the continent level, Asia, Europe, and North America are very close to each other, while Australia, Africa and South America are differentiated (Fig. 7a). The differentiation between eight hydrobelts is much greater (Fig. 7b),

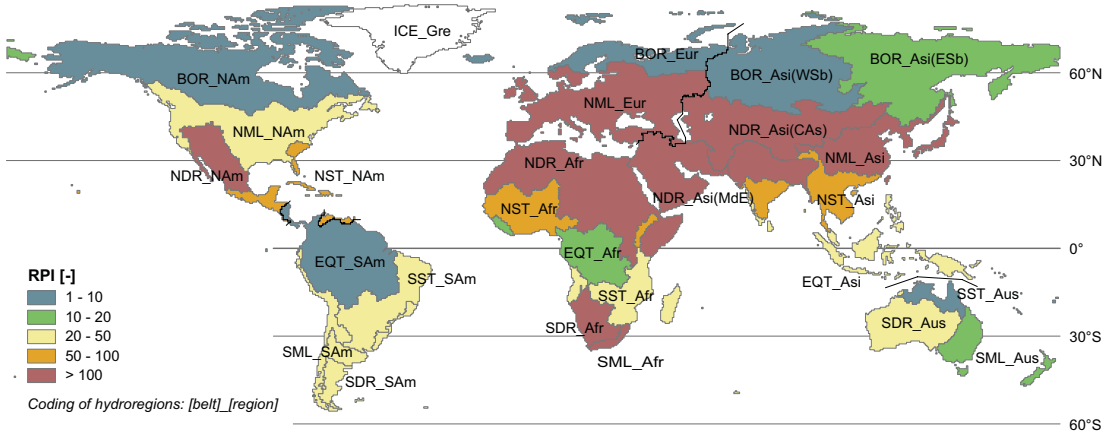

Fig. 6. Global distribution of the relative population pressure (RPI) indicator at hydroregion level (see Sect. 4.2). RPI = (d_{pop}/q)hydroregion/(d_{pop}/q) N. Am boreal region.

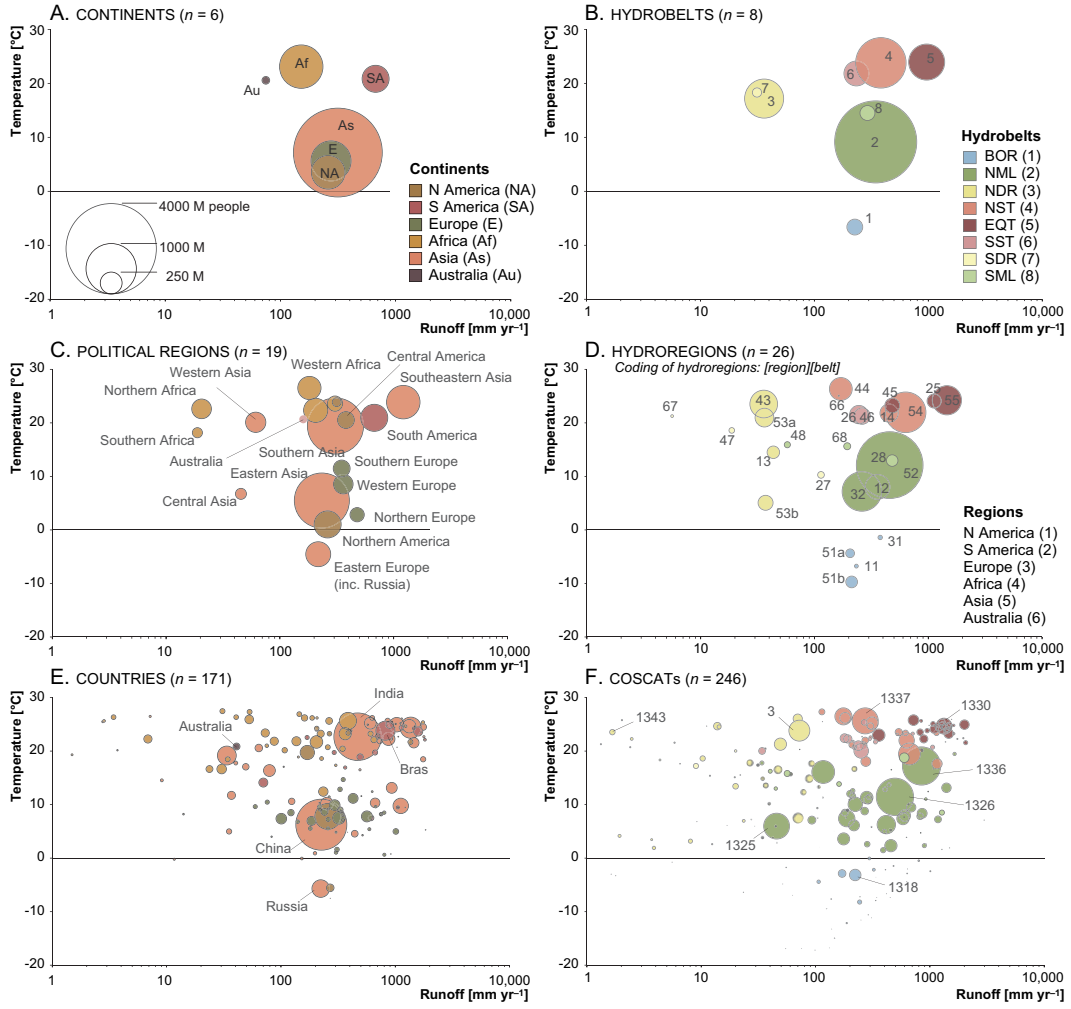

Fig. 7. Bubble chart of populations represented in a run-off vs. temperature domain. **(a)** Reporting using continents; **(b)** hydrobelts; **(c)** political regions; **(d)** hydroregions; **(c)** countries; **(f)** Coastal catchments (COSCATs); COSCAT numbers from Meybeck et al. (2006)) (30′ cell averages of annual figures for temperatures and run-off).

and three clusters of population under severe hydroclimatic stress are well identified: the boreal hydrobelt, where 123 million people live at negative temperatures, $-8\,^{\circ}\mathrm{C}$ on average, and the north and south dry hydrobelts with 740 million people that live under potential water shortage, with only $35\,\mathrm{mm\,yr^{-1}}$ on average.

When we compare the hydroregion level of aggregation ($n = 26$) to the UN economic regions ($n = 19$) (United Nations, 2000) (Fig. 7c, d), the following appears: on both scales the population distribution is more differentiated than in hydrobelt and continent cases. Many differences are noted as (i) the overestimation of population living in cold areas, when Eastern Europe is mixed with Siberia, and the population living with run-off less than $20\,\mathrm{mm\,yr^{-1}}$; (ii) a biased message provided for highly heterogeneous regions/countries in Australia, Northern America (excluding Central America) or South America. At such scale the hydroregions are generally performing well for a global analysis.

Local analysis is often made at the country level ($n = 171$; Fig. 7e). It is here compared with coastal catchments ($n = 246$, here including additional endorheic entities; Fig. 7f). At such scale the overall global picture is difficult to decipher and the bubble size, i.e. the population, limits the visualisation. In the biggest countries, the population is not well represented in the T vs. q domain: it is too cold for most Russians, too dry for most Chinese, too wet for most Brazilians. At this scale the coastal catchments provide a better scale for reporting. For instance, the hydroclimate conditions of Huang He (Yellow River; COSCAT # 1325) are well separated from other Chinese coastal catchments (Yangtze, # 1326). In some hydrobelts (BOR, EQT, NST, SST), the coastal catchments are well clustered in such a representation. For the northern mid-latitude and the dry belts, they are more dispersed.

5 Conclusions and perspectives

In this paper, we presented the hydrobelt/hydroregion concept, designed for the analysis and reporting of water-related issues. Using three criteria, based purely on hydrophysical features (average temperature, run-off, and basin boundaries), we divided the world into eight hydrobelts, which are hydrologically as homogenous as possible, while the interbelt differences are maximised. The hydroclimates are relatively similar within a single belt and in the analogues found in the Northern or Southern Hemisphere. The hydrobelts sufficiently take into account many important physical features of the Earth system and hydrological concepts such as endorheism/exorheism, arheism and the former glacial cover of river basins.

Hydrobelts are represented on the continents by 26 hydroregions. At this level the global distribution of population is very contrasted due to the history of global demography: (i) the belts in the Northern Hemisphere are more heavily populated than their counterparts in the Southern Hemisphere; (ii) the hydroregions of the "Old World" are much more populous than those of the "New World"; (iii) the Australian hydroregions are much less populated than all other similar hydroregions; (iv) the hydroregions of the boreal belt are the least populated. The distribution of average population density varies over two orders of magnitude when analysed at the level of hydroregions.

When applying hydrobelts and hydroregions to the population pressure on river run-off, using a simple, dimensionless indicator, we can scale and identify the populations and regions at risk of severe degradation of water quality if no remedial measures are taken. Our analysis also shows higher differentiations compared to many conventional aggregations, e.g. those done using continental or political delineations.

We argue, therefore, that hydrobelts and hydroregions could be, in many cases, more appropriate for the global-scale reporting of water-related issues, compared to the more conventionally used continents or other non-physical regional aggregations. Hydrobelts and hydroregions are also suitable when the global analyses of water issues require fixed river basin boundaries, which is unlikely to change within the coming decades. These analyses include, for example, climate change impacts, relationships between basins and population, water management, aquatic biodiversity, river fluxes and basin yields, and their alteration by humans. The double reporting level – eight hydrobelts or twenty-six hydroregions – also offers flexibility when tabulating and reporting the global-scale analyses.

Supplementary material related to this article is available online at: http://www.hydrol-earth-syst-sci.net/17/1093/2013/hess-17-1093-2013-supplement.zip.

Acknowledgements. MK received funding from Aalto University Postdoctoral research fund. HHD received funding from NSERC (Canada Excellence Research Chair in Ecohydrology – Philippe van Cappellen) and Utrecht University high potential programme (G-NUX project; awarded to Hans Middelkoop and Caroline Slomp). We thank Olli Varis for his support and helpful comments. The constructive and thoughtful comments of the two reviewers are highly appreciated.

Edited by: R. Woods

References

Abell, R., Thieme, M. L., Revenga, C., Bryer, M., Kottelat, M., Bogutskaya, N., Coad, B., Mandrak, N., Balderas, S. C., Bussing, W., Stiassny, M. L. J., Skelton, P., Allen, G. R., Unmack, P., Naseka, A., Ng, R., Sindorf, N., Robertson, J., Armijo, E., Higgins, J. V., Heibel, T. J., Wikramanayake, E., Olson, D., López,

H. L., Reis, R. E., Lundberg, J. G., Sabaj Pérez, M. H., and Petry, P.: Freshwater Ecoregions of the World: A New Map of Biogeographic Units for Freshwater Biodiversity Conservation, BioScience, 58, 403–414, doi:10.1641/b580507, 2008.

Alcamo, J., Döll, P., Henrichs, T., Kaspar, F., Lehner, B., Rösch, T., and Siebert, S.: Development and testing of the WaterGAP 2 global model of water use and availability, Hydrol. Sci. J., 48, 317–338, 2003.

Alcamo, J., Flörke, M., and Märker, M.: Future long-term changes in global water resources driven by socio-economic and climatic changes, Hydrol. Sci. J., 52, 247–275, 2007.

Arnell, N. W.: Climate change and global water resources: SRES emissions and socio-economic scenarios, Global Environ. Change, 14, 31–52, 2004.

Baumgartner, A. and Reichel, E.: The World Water Balance, Elsevier, 179 pp., 1975.

Brown, J., Ferrians Jr., O. J., Heginbottom, J. A., and Melnikov, E. S.: (revised February 2001) Circum-Arctic map of permafrost and ground-ice conditions, National Snow and Ice Data Center/World Data Center for Glaciology. Digital Media. Data downoaded from: http://rims.unh.edu/data/data.cgi (last access: 29 August 2011, Boulder, CO, 1998.

Costard, F., Gautier, E., Brunstein, D., Hammadi, J., Fedorov, A., Yang, D., and Dupeyrat, L.: Impact of the global warming on the fluvial thermal erosion over the Lena river in Central Siberia, Geophys. Res. Lett., 34, L14501, doi:10.1029/2007GL030212, 2007.

Cruette, J. and Rodier, J. A.: Mesures de débits de l'Oued Zeroud pendant les crues exceptionneles de l'Automne 1969, Cahiers ORSTOM, Série Hydrologie, 13, 33–64, 1971.

Dukhovny, V. A. and De Schutter, J.: Water in Central Asia: Past, Present and Future, CRC Press Inc, 432 pp., 2011.

Dürr, H. H.: Vers une typologie des systèmes fluviaux à l'échelle globale: quelques concepts et exemples à résolution moyenne, Université Paris VI – Pierre et Marie Curie, 721 pp., 2003.

Dürr, H. H., Meybeck, M., and Dürr, S. H.: Lithologic composition of the Earth's continental surfaces derived from a new digital map emphasizing riverine material transfer, Global Biogeochem. Cy., 19, GB4S10, doi:10.1029/2005GB002515, 2005.

Dürr, H., Laruelle, G., van Kempen, C., Slomp, C., Meybeck, M., and Middelkoop, H.: Worldwide Typology of Nearshore Coastal Systems: Defining the Estuarine Filter of River Inputs to the Oceans, Estuar. Coast., 34, 441–458, doi:10.1007/s12237-011-9381-y, 2011.

Fairbridge, R. (Ed): The Encyclopedia of Geomorphology, Van Nostrand Rheinhold, New York, 1321, 1972.

Falkenmark, M.: Meeting water requirements of an expanding world population, Philos. Trans. R. Soc. Lond B. Biol Sci., 352, 929–936, doi:10.1098/rstb.1997.0072, 1997.

Falkenmark, M. and Lindh, G.: How can we cope with the water resources situation by the year 2015, Ambio, 3, 114–122, 1974.

Falkenmark, M., Lundqvist, J., and Widstrand, C.: Macro-scale water scarcity requires micro-scale approaches, Nat. Resour. Forum, 13, 258–267, 1989.

Falkenmark, M., Rockström, J., and Karlberg, L.: Present and future water requirements for feeding humanity, Food Security, 1, 59–69, doi:10.1007/s12571-008-0003-x, 2009.

Fekete, B. M., Vörösmarty, C. J., and Grabs, W.: High-resolution fields of global runoff combining observed river discharge and simulated water balances, Global Biogeochem. Cy., 16, 1042, doi:1010.1029/1999GB001254, 2002.

Gerasimov, G. N. et al. (Eds): Physico-Geographical World Atlas, Scientific Academy of URSS and Cartographic and Geodesic Central Committee, Moscow, 298 pp., 1964.

Haines, A. T., Finlayson, B. L., and McMahon, T. A.: A global classification of river regimes, Appl. Geogr., 8, 255–272, 1988.

Hijmans, R. J., Cameron, S. E., Parra, J. L., Jones, P. G., and Jarvis, A.: Very high resolution interpolated climate surfaces for global land areas, Int. J. Climatol., 25, 1965–1978, 2005.

Holdridge, L. R.: Life Zone Ecology, Tropical Science Center, San José, 1967.

Islam, S., Oki, T., Kanae, S., Hanasaki, N., Agata, Y., and Yoshimura, K.: A grid-based assessment of global water scarcity including virtual water trading, Water Resour. Manage., 21, 19–33, 2007.

Kabat, P., Claussen, M., Dirmeyer, P. A., Gash, J. H. C., BravodeGuenni, L., Meybeck, M., Pielke, R. S., Vörösmarty, C. J., Hutjes, R. W. A., and Lütkemeier, S. (Eds.): Vegetation, Water, Humans and the Climate. A New Perspective on an Interactive System, Global Change – The IGBP Series, Springer, 566 pp., 2004.

Klein Goldewijk, K., Beusen, A., and Janssen, P.: Long-term dynamic modeling of global population and built-up area in a spatially explicit way: HYDE 3.1, The Holocene, 20, 565–573, 2010.

Köppen, W.: Das Geographische System der Klimate, Handbuch der Klimatologie, Berlin, Germany, 1931.

Korzoun, V. I., Sokolov, A. A., Budyko, M. I., Voskresensky, K. P., Kalinin, G. P., Konoplyantsev, A. A., Korotkevich, E. S., and L'vovich, M. I.: Atlas of World Water Balance and Water Resources of the Earth, USSR Committee for the International Hydrological Decade. Studies and Reports in Hydrology 25, Unesco, Paris, 663 pp., Leningrad, 1978.

Kotwicki, V.: Floods of Lake Eyre, Engineering and Water Supply Department, Adelaide, 99 pp., 1986.

Kulshreshtha, S. N.: A Global Outlook for Water Resources to the Year 2025, Water Resour. Manage., 12, 167–184, doi:10.1023/a:1007957229865, 1998.

Kummu, M. and Varis, O.: The World by latitudes: a global analysis of human population, development level and environment across the north-south axis over the past half century, Appl. Geogr., 31, 495–507, doi:10.1016/j.apgeog.2010.10.009, 2011.

Kummu, M., Ward, P. J., de Moel, H., and Varis, O.: Is physical water scarcity a new phenomenon? Global assessment of water shortage over the last two millennia, Environ. Res. Lett., 5, 034006, doi:10.1088/1748-9326/5/3/034006, 2010.

Kummu, M., de Moel, H., Ward, P. J., and Varis, O.: How close do we live to water? A global analysis of population distance to freshwater bodies, PLoS ONE, 6, e20578, doi:10.1371/journal.pone.0020578, 2011.

Laruelle, G. G., Dürr, H. H., Slomp, C. P., and Borges, A. V.: Evaluation of sinks and sources of CO_2 in the global coastal ocean using a spatially-explicit typology of estuaries and continental shelves, Geophys. Res. Lett., 37, L15607, doi:10.1029/2010gl043691, 2010.

Leemans, R.: Global Holdridge Life Zone Classifications, in: Global Ecosystems Database Version 2.0, NOAA National Geophysical Data Center, Boulder, Colorado, USA, 1992.

Lehner, B. and Döll, P.: Development and validation of a global database of lakes, reservoirs and wetlands, J. Hydrol., 296, 1–22, 2004.

Ludwig, W. and Probst, J.-L.: River sediment discharge to the oceans: present-day controls and global budgets, Am. J. Sci., 298, 265–295, 1998.

McNeill, J. R. and McNeill, W. H.: The Human Web: A Bird's-Eye View of World History, W. W. Norton & Company, 368 pp., 2003.

Meybeck, M.: How to establish and use world budgets of riverine materials, in: Physical and chemical weathering in geochemical cycles, edited by: Lerman, A. and Meybeck, M., Kluwer Academic Publishers, Dordrecht, 247–272, 1988.

Meybeck, M.: Global analysis of river systems: from earth system controls to Anthropocene controls, Phil. Trans. Royal Acad. London B, 358, 1935–1955, 2003.

Meybeck, M. and Dürr, H. H.: Cascading Filters of River Material from Headwaters to Regional Seas: The European Example, in: Watersheds, Bays, and Bounded Seas – The Science and Management of Semi-Enclosed Marine Systems, edited by: Urban, E. R. J., Sundby, B., Malanotte-Rizzoli, P., and Melillo, J. M., SCOPE Series, Island Press, Washington, 115–139, 2009.

Meybeck, M. and Helmer, R.: The quality of rivers: from pristine stage to global pollution, Global Planet. Change, 1, 283–309, 1989.

Meybeck, M. and Ragu, A.: GEMS/Water Contribution to the Global Register of River Inputs (GLORI), Provisional Final Report, UNEP/WHO/UNESCO, Geneva, 245 pp., 1995.

Meybeck, M., Dürr, H. H., and Vörösmarty, C. J.: Global coastal segmentation and its river catchment contributors: a new look at land-ocean linkage, Global Biogeochem. Cy., 20, GB1S90, doi:10.1029/2005GB002540, 2006.

Meybeck, M., Dürr, H. H., Roussennac, S., and Ludwig, W.: Regional Seas and their interception of riverine fluxes to oceans, Mar. Chem., 106 (Wollast Memorial Special Issue), 301–325, 2007.

Millennium Ecosystem Assessment: Ecosystems and Human Well-being: Synthesis, Island Press, Washington, DC, 155 pp., 2005.

Milliman, J. D. and Farnsworth, K. L.: River Discharge to the Coastal Ocean – A Global Synthesis, Cambridge University Press, New York, 2011.

Nilsson, C., Reidy, C. A., Dynesius, M., and Revenga, C.: Fragmentation and flow regulation of the world's large river systems, Science, 308, 405–408, 2005.

Nyamweru, C.: New evidence for the former extent of the Nile drainage system, The Geographical Journal, 155, 179–188, 1989.

Oki, T. and Kanae, S.: Global Hydrological Cycles and World Water Resources, Science, 313, 1068–1072, doi:10.1126/science.1128845, 2006.

Petit-Maire, N. and Guo, Z. T.: Mid-Holocene climatic change and man in the present-day Sahara desert, Quaternary Deserts and Climatic Change, Al Ain/United Arab Emirates, 351–356, 1995.

Potter, P. E.: Petrology and chemistry of modern big river sands, J. Geol., 86, 423–449, 1978.

Potter, P. E. and Hamblin, W. K.: Big Rivers Worldwide, Brigham Young University, Geology Studies, Provo,Utah, p. 78, 2006.

Probst, J.-L.: Géochimie et Hydrochimie de l' érosion continentale. Mécanismes, bilan global actuel et fluctuations au cours des 500 derniers millions d'années, Sciences Géologiques Mémoires 94, Strasbourg, 161 pp., 1992.

Probst, J. L., Ludwig, W., and Amiotte-Suchet, P.: Global modelling of CO_2 uptake by continental erosion and of carbon river transport to the oceans, Sci. Geol. Bullet., 50, 131–156, 1997.

Rockström, J., Falkenmark, M., Karlberg, L., Hoff, H., Rost, S., and Gerten, D.: Future water availability for global food production: The potential of green water for increasing resilience to global change, Water Resour. Res., 45, W00A12, doi:10.1029/2007WR006767, 2009.

Rodier, J. A.: Régimes hydrologiques de l'Afrique Noire à l'ouest du Congo, Mém. Orstom, Paris, 137 pp., 1964.

Rubel, F. and Kottek, M.: Observed and projected climate shifts 1901-2100 depicted by world maps of the Köppen-Geiger climate classification, Meteorologische Z., 19, 135–141, 2010.

Said, R.: The River Nile – Geology, Hydrology and Utilisation, 1st Edn., Pergamon Press, Oxford, New York, Seoul, Tokyo, 320 pp., 1993.

Salomons, W., Kremer, H., and Turner, K.: The catchment to coast continuum, in: Coastal fluxes in the Athropocene, edited by: Crossland, C. J., Kremer, H. H., Lindeboom, H. J., Marshall Crossland, J. J., and Le Tissier, M. D. A., Springer, 145–200, 2005.

Sarnthein, M., Seibold, E., and Rognon, P. (Eds.): Sahara and surrounding seas: sediments and climatic changes, Palaeoecology of Africa and the surrounding islands, edited by: van Zinderen Bakker Sr, E. M. and Coetzee, J. A., Balkema, A. A., Rotterdam, 1980.

Schultz, J.: The ecozones of the World, Springer, 252 pp., 2005.

Seitzinger, S. P., Harrison, J. A., Dumont, E., Beusen, A. H. W., and Bouwman, A. F.: Sources and delivery of carbon, nitrogen, and phosphorus to the coastal zone: an overview of Global Nutrient Export from Watersheds (NEWS) models and their application, Global Biogeochem. Cy., 19, GB4S01, doi:10.1029/2005GB002606, 2005.

Seitzinger, S. P., Mayorga, E., Bouwman, A. F., Kroeze, C., Beusen, A. H. W., Billen, G., Drecht, G. V., Dumont, E., Fekete, B. M., Garnier, J., and Harrison, J. A.: Global river nutrient export: A scenario analysis of past and future trends, Global Biogeochem. Cy., 24, GB0A08, doi:10.1029/2009GB003587, 2010.

Steffen, W., Sanderson, A., Tyson, P. D., Jäger, J., Matson, A., Moore, B., Oldfield, F., Richardson, K., Schellnhuber, H. J., Turner, B. I., and Wasson, R. J. (Eds.): Global Change and the Earth System: a Planet Under Pressure, Springer, Berlin, 2004.

Sullivan, C. A., Meigh, J. R., Giacomello, A. M., Fediw, T., Lawrence, P., Samad, M., Mlote, S., Hutton, C., Allan, J. A., Schulze, R. E., Dlamini, D. J. M., Cosgrove, W., Priscoli, J. D., Gleick, P., Smout, I., Cobbing, J., Calow, R., Hunt, C., Hussain, A., Acreman, M. C., King, J., Malomo, S., Tate, E. L., O'Regan, D., Milner, S., and Steyl, I.: The Water Poverty Index: Development and application at the community scale, Nat. Resour. Forum, 27, 189–199, 2003.

Talaue-McManus, L., Smith, S. V., and Buddemeier, R. W.: Biophysical and socio-economic assessments of the coastal zone: the LOICZ approach, Ocean Coast. Manage., 46, 323–333, 2003.

Tedesco, P. A., Hugueny, B., Oberdorff, T., Dürr, H. H., Mérigoux, S., and de Mérona, B.: River hydrological seasonality influences life history strategies of tropical riverine fishes, Oecologia, 156, 691–702, doi:10.1007/s00442-008-1021-2, 2008.

van Beek, L. P. H., Wada, Y., and Bierkens, M. F. P.: Global monthly water stress: 1. Water balance and water availability, Water Resour. Res., 47, W07517, doi:10.1029/2010wr009791, 2011.

Viviroli, D., Dürr, H. H., Messerli, B., Meybeck, M., and Weingartner, R.: Mountains of the world – water towers for humanity: typology, mapping and global significance, Water Resour. Res., 43, W07447, doi:10.1029/2006WR005653, 2007.

Vörösmarty, C. J., Sharma, K., Fekete, B., Copeland, A. H., Holden, J., Marble, J., and Lough, J. A.: The storage and aging of continental runoff in large reservoir systems of the world, Ambio, 26, 210–219, 1997.

Vörösmarty, C. J., Fekete, B. M., Meybeck, M., and Lammers, R. B.: Geomorphometric attributes of the global system of rivers at 30-minute spatial resolution, J. Hydrol., 237, 17–39, 2000a.

Vörösmarty, C. J., Fekete, B. M., Meybeck, M., and Lammers, R. B.: The global system of rivers: its role in organizing continental land mass and defining land-to-ocean linkages, Global Biogeochem. Cy., 14, 599–621, 2000b.

Vörösmarty, C. J., Green, P., Salisbury, J., and Lammers, R. B.: Global Water Resources: Vulnerability from Climate Change and Population Growth, Science, 289, 284–288, 2000c.

Vörösmarty, C. J., McIntyre, P. B., Gessner, M. O., Dudgeon, D., Prusevich, A., Green, P., Glidden, S., Bunn, S. E., Sullivan, C. A., Liermann, C. R., and Davies, P. M.: Global threats to human water security and river biodiversity, Nature, 467, 555–561, doi:10.1038/nature09440, 2010.

Wada, Y., Beek, L. P. H. v., Viviroli, D., Dürr, H. H., Weingartner, R., and Bierkens, M. F. P.: Global monthly water stress: 2. Water demand and severity of water stress, Water Resour. Res., 47, W07518, doi:10.1029/2010WR009792, 2011.

World Water Assessment Programme: The United Nations World Water Development Report 3: Water in a Changing World, Paris: UNESCO, and London: Earthscan, 2009.